

See discussions, stats, and author profiles for this publication at: <https://www.researchgate.net/publication/319235591>

Optimal Water–Power Flow Problem: Formulation and Distributed Optimal Solution

Article in IEEE Transactions on Control of Network Systems · August 2017

DOI: 10.1109/TCNS.2018.2792699

CITATIONS

125

READS

788

5 authors, including:



Ahmed S Zamzam

National Renewable Energy Laboratory

73 PUBLICATIONS 1,388 CITATIONS

SEE PROFILE



N.D. Sidiropoulos

University of Minnesota

390 PUBLICATIONS 22,574 CITATIONS

SEE PROFILE

Optimal Water-Power Flow Problem: Formulation and Distributed Optimal Solution

Ahmed S. Zamzam, Emiliano Dall’Anese, Changhong Zhao, Josh A. Taylor, and
Nicholas D. Sidiropoulos

Abstract

This paper formalizes an optimal water-power flow (OWPF) problem to optimize the use of controllable assets across power and water systems while accounting for the couplings between the two infrastructures. Tanks and pumps are optimally managed to satisfy water demand while improving power grid operations; for the power network, an AC optimal power flow formulation is augmented to accommodate the controllability of water pumps. Unfortunately, the physics governing the operation of the two infrastructures and coupling constraints lead to a nonconvex (and, in fact, NP-hard) problem; however, after reformulating OWPF as a nonconvex, quadratically-constrained quadratic problem, a feasible point pursuit-successive convex approximation approach is used to identify feasible and optimal solutions. In addition, a distributed solver based on the alternating direction method of multipliers enables water and power operators to pursue individual objectives while respecting the couplings between the two networks. The merits of the proposed approach are demonstrated for the case of a distribution feeder coupled with a municipal water distribution network.

A. S. Zamzam is with the Department of Electrical and Computer Engineering, University of Minnesota, Minneapolis, MN 55455, USA. Emails: ahmedz@umn.edu

E. Dall’Anese and C. Zhao are with the National Renewable Energy Laboratory, Golden, CO 80401, USA. Emails: {emiliano.dallanese, changhong.zhao}@nrel.gov

J. A. Taylor is with the Department of Electrical and Computer Engineering, University of Toronto, Toronto, ON M5S 3G4, Canada. Email: josh.taylor@utoronto.ca

N. D. Sidiropoulos is with the Department of Electrical and Computer Engineering, University of Virginia, Charlottesville, VA 22904, USA. Email: nikos@virginia.edu

The work of A.S. Zamzam and N.D. Sidiropoulos was partially supported by NSF under grant CIF-1525194. The work of E. Dall’Anese and C. Zhao was supported in part by the Laboratory Directed Research and Development program at the National Renewable Energy Laboratory.

Index Terms

Power systems, water systems, optimal power flow, optimal water flow, successive convex approximation, distributed algorithms.

I. INTRODUCTION

Power and water networks are critical infrastructures. These systems are predominantly planned and operated independently, although their operation is intrinsically coupled at multiple spatial and temporal scales. For example, electric pumps for agricultural and municipal water systems affect the operation (in the form of power and energy demands) of power distribution grids [1]–[3]; on the other hand, the capacity of thermoelectric power plants strongly depends on the availability of cooling water [4]–[6]. With reference to municipal and wastewater systems, electric pumps are key elements to overcoming geographical differences in head pressure and head losses caused by pipe friction, and they enable the supply of water demand within given water quality standards. Electricity consumption from pumps constitutes major operating costs for water utilities. For example, in the United States the overall operation of drinking and wastewater networks represents 4% of the total electricity consumption [7]. Optimizing water pump operation has therefore significant potential to save energy, reduce emissions, and enhance the reliability and efficiency of the power grid.

Under dynamic electricity pricing, water utilities can schedule their pumps and adjust the consumption of variable-speed-drive pumps to minimize the cost of energy. The optimal pump scheduling problem is often formulated as a (nonconvex) mixed integer nonlinear program (MINLP), wherein nonlinearity stems from the water network hydraulic model, and binary variables indicate the pumps' on/off status. In the literature, various approaches have been developed for MINLPs. These include (piecewise) linear approximations [8]–[11], nonconvex nonlinear programming relaxation [12], continuous constraint relaxation combined with branch and bound [13], hydraulic simulation to implicitly enforce nonlinear constraints [14], Lagrange decomposition integrated with simulation-based search [15], gradient method together with sensitivity analysis [16], and problem-specific presolving techniques [17]. Finally, [18] bypasses the nonlinearity of the water network hydraulic model by leveraging a second-order cone relaxation, and sufficient conditions for the exactness of the relaxation are provided. Optimizing the operation of municipal water distribution networks in response to time-varying electricity prices was also

considered in [19]. A two-step approach is taken whereby the operation of the water network is optimized *a priori*, and the controllable assets in the power network are then optimized in a subsequent stage based on the consumption of the water pumps.

A variety of additional objectives and constraints can arise when optimizing the operation of water pumps. Examples include the cost of energy loss caused by pipe friction [18], maximum electricity demand charges (together with unit charges) [16], peak power consumption, maintenance costs, reservoir level variation [20], and land subsidence [21]. Another line of work focuses on dynamic optimal pump management, which is usually formulated as a dynamic programming problem [22]–[24]. A difficulty is to obtain a near optimal solution of the dynamic program in a reasonable amount of time. To overcome this challenge, techniques such as simplifying hydraulic dynamics [24], spatial decomposition of water networks, and temporal decomposition of operation periods [22], [23] are exploited in formulating and solving the dynamic program.

The works mentioned above pertain to optimal management of water networks, and the main interaction with power systems—if any—is in the form of responsiveness to electricity prices. It is, however, increasingly recognized that a *joint* optimization of power and water infrastructures can bring significant benefits from operational and economical standpoints [25]. Controllable assets of water utilities can provide valuable services to power systems to enhance reliability and efficiency, as well as to cope with the volatility of distributed renewable generation; these services include frequency regulation, regulating reserves, and contingency reserves. On the other hand, the incentives for the provisioning of grid services to electric utilities could be used by water system operators for capital improvements and capacity expansion. To the best of our knowledge, however, there are no systematic approaches to jointly optimize the use of controllable assets across power and water systems while acknowledging intrinsic couplings between the two infrastructures.

This paper formulates an optimal water-power flow (OWPF) problem to minimize the (sum of the) cost functions associated with water and power operators while respecting relevant engineering and operational constraints of the two systems as well as pertinent intra-system coupling constraints. In particular, the power consumed by a pump is related to the pump’s pressure gain and flow rate. The problem is tailored to coupled power distribution feeders and municipal water distribution networks (although its applicability is not limited to this operational setting), and it addresses the controllability of distributed energy resources (DERs) and water

pumps. Pump selection is not addressed because it is assumed that a pump scheduling problem is solved at a slower timescale than the OWPF. Because of the AC power flow equations and the water network hydraulic model, the OWPF problem is nonconvex (and NP-hard).

The proposed technical approach involves the reformulation of nonconvex constraints as equivalent nonconvex quadratic constraints, thus leading to an equivalent OWPF problem that is in the prototypical form of a nonconvex quadratically constrained quadratic program (QCQP). The resulting nonconvex QCQP is then solved by using the feasible point pursuit-successive convex approximation (FPP-SCA) method [26], [27]. The FPP-SCA algorithm replaces the nonconvex constraints by inner convex surrogates around a specific point to construct a convex restriction of the original problem. Because such restriction might lead to infeasibility, the main operating principles of the algorithm to identify a feasible and optimal point involve the following two phases:

- 1) *Feasibility phase*: a feasible solution is obtained by solving a sequence of approximations of the original problem, where slack variables are added after restriction to quantify and ultimately zero-out the amount of constraint violations;
- 2) *Refinement phase*: successive convex approximation of the feasible set is used to find a Karush-Kuhn-Tucker (KKT) point of the OWPF problem.

One of the practical challenges of the solution outlined above is the need for a centralized computational platform that can solve the OWPF problem. To bypass the need for a central controller, we develop a distributed solver based on the alternating direction method of multipliers [28]. With the distributed solution method, water and power operators can pursue individual operational objectives and retain controllability of their own assets (pumps for the water network and DERs for the power network) while respecting operational couplings between the two networks [25]. In the resulting iterative procedure, each system operator solves a smaller optimization problem with variables associated only with its network and controllable devices; water and power operators subsequently exchange information regarding the shared variables to *reach consensus* on the powers consumed by the water pumps. This represents an additional unique contribution of the present paper.

Centralized and distributed methods are tested using an IEEE distribution test feeder connected to a municipal water distribution network adopted from the literature.

It is worth pointing out that for the AC optimal power flow problem, a number of approaches

have been proposed in the literature based on semidefinite relaxations, second-order cone relaxation, and linearization methods for the AC power flow equations; see, for example, [29]–[35] and pertinent references therein. In this paper, we adopt the FPP-SCA method [27] because it allows us to tackle the nonconvexity of constraints of both water and power networks in a unified manner.

The rest of this paper is organized as follows. Section II contains the modeling of a municipal water network, and Section III introduces the model for the power distribution network. Section IV outlines the proposed OWPF problem is outlined. Section V illustrates the application of the FPP-SCA approach to the joint optimization problem, and Section VI presents the distributed algorithm. Section VII demonstrates the effectiveness of the proposed algorithm via a test case from the literature, and Section VIII summarizes conclusions and findings.

Notation: matrices (vectors) are denoted by boldface capital (small) letters unless otherwise stated; $(\cdot)^T$, $(\cdot)^*$, and $(\cdot)^H$ stand for transpose, conjugate, and complex-conjugate transpose, respectively; and $|\cdot|$ denotes the magnitude of a number or the cardinality of a set.

II. MODELING THE WATER NETWORK

As in [18], we consider a municipal water network comprising a set of nodes \mathcal{N} and a set of pipes \mathcal{L} linking the nodes. The disjoint sets \mathcal{J} , \mathcal{T} , and \mathcal{R} , with $\mathcal{N} = \mathcal{J} \cup \mathcal{T} \cup \mathcal{R}$, denote the sets of junctions, tanks, and reservoirs, respectively. The disjoint subsets \mathcal{P} and \mathcal{V} of \mathcal{L} have variable-speed pumps and pressure-reducing valves, respectively. We optimize the water system operation during an interval $t = 1, \dots, T$, with δ representing the time interval between two consecutive time periods. We assume that the on/off states of the pumps and valves are determined at a slower timescale and hence constant over $t = 1, \dots, T$. Note that water can only flow in one direction through a pump or a valve. Moreover, we assume that the directions of water flow in pipes without pumps or valves do not change over $t = 1, \dots, T$. Therefore, $(\mathcal{N}, \mathcal{L})$ can be modeled as a *directed* graph, wherein \mathcal{P} and \mathcal{V} are the sets of pipes with pumps and valves that are in an “on” state during $t = 1, \dots, T$, respectively. Let q_{ij}^t denote the volumetric water flow rate through a pipe $ij \in \mathcal{L}$ at time $t = 1, \dots, T$. Next, we list the models for different components in water networks. Fig. 1 illustrates an example of water network taken from [36]; the network features 7 junctions, 2 reservoirs, a tank, 3 pumps, and 2 valves. This network will be utilized in the numerical experiments in Section VII.

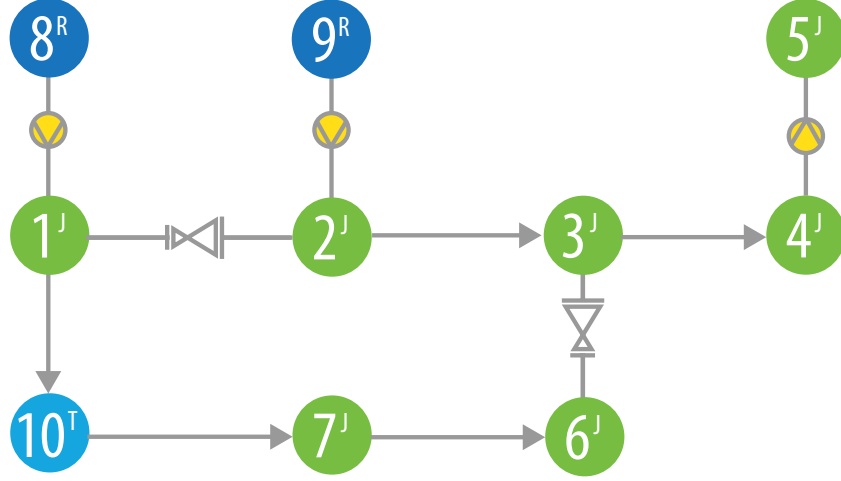


Fig. 1. Example of municipal water network [36]; this network will be utilized in the numerical experiments.

Junctions: Denote the water demand at junction $j \in \mathcal{J}$ at time t as d_j^t . Then, the following mass conservation constraint must hold:

$$\sum_{i:ij \in \mathcal{L}} q_{ij}^t - \sum_{k:j \in \mathcal{L}} q_{jk}^t = d_j^t, \quad \forall j \in \mathcal{J}, \quad \forall t = 1, \dots, T. \quad (1)$$

The head pressure at junction $j \in \mathcal{J}$ at time interval t , denoted by h_j^t , must satisfy the condition:

$$h_j^t \geq h_j^{\min}, \quad \forall j \in \mathcal{J}, \quad \forall t = 1, \dots, T \quad (2)$$

where h_j^{\min} is the minimum allowable pressure head at junction j (assigned by the water system operator based on engineering considerations).

Tanks: Let μ_k^t denote the volume of water in a tank $k \in \mathcal{T}$ at time t . The pressure head $h_k^{t,\text{out}}$ at the outlet of tank k at time t satisfies the equation $A_k h_k^{t,\text{out}} = \mu_k^t$, where the constant A_k denotes the cross-sectional area of tank k . Further, the tank outlet pressure heads satisfy the following constraints:

$$h_k^{t,\text{out}} = h_k^{t-1,\text{out}} + \frac{\delta}{A_k} \left(\sum_{i:ik \in \mathcal{L}} q_{ik}^t - \sum_{j:kj \in \mathcal{L}} q_{kj}^t \right) \quad (3)$$

$$0 \leq h_k^{t,\text{out}} \leq h_k^{t,\text{in}}, \quad \forall k \in \mathcal{T}, \quad \forall t = 1, \dots, T \quad (4)$$

with the initial pressure head $h_k^{0,\text{out}}$ determined based on the initial volume μ_k^0 as $h_k^{0,\text{out}} = \mu_k^0/A_k$. The inlet pressure head $h_k^{t,\text{in}}$ is a variable that can be adjusted to determine the inlet flow rate. An upstream node of tank k sees its inlet head $h_k^{t,\text{in}}$, whereas a downstream node sees its outlet head $h_k^{t,\text{out}}$. In the sequel, for notational simplicity, we use only h_k^t to denote $h_k^{t,\text{in}}$ in an equation related to an upstream node, and $h_k^{t,\text{out}}$ in an equation related to a downstream node. In Fig. 1, the tank corresponds to node 10.

Reservoirs: We treat the reservoirs $r \in \mathcal{R}$ as infinite sources of water where the mass conservation constraint (1) is not imposed. The pressure heads at reservoirs are set to zero:

$$h_r^t = 0, \quad \forall r \in \mathcal{R}, \quad \forall t = 1, \dots, T. \quad (5)$$

The reservoirs in Fig. 1 are color-coded in blue and are located at nodes 8 and 9.

Variable-speed pumps: The pressure head gain due to a variable-speed pump, which is denoted by \hat{h}_{ij}^t , is modeled as [37], [38]:

$$\hat{h}_{ij}^t = A_{ij} (q_{ij}^t)^2 + B_{ij} q_{ij}^t w_{ij}^t + C_{ij} (w_{ij}^t)^2 \quad (6)$$

$$0 \leq w_{ij}^t \leq w_{ij}^{\max}, \quad \forall ij \in \mathcal{P}, \quad \forall t = 1, \dots, T \quad (7)$$

where w_{ij}^t and w_{ij}^{\max} are the ratio of the actual pump speed to the nominal speed and the maximum allowable w_{ij}^t , respectively. The coefficients $A_{ij} \leq 0$, $B_{ij} \geq 0$, and $C_{ij} \geq 0$ are pump parameters evaluated at the nominal speed. The following constraints hold for the pumps with an “on” state:

$$\hat{h}_{ij}^t = (h_j^t + \bar{h}_j) - (h_i^t + \bar{h}_i) \quad (8)$$

$$\hat{h}_{ij}^t \geq 0 \quad (9)$$

$$q_{ij}^t \geq 0, \quad \forall ij \in \mathcal{P}, \quad \forall t = 1, \dots, T \quad (10)$$

where \bar{h}_i denotes the elevation of node i . In Fig. 1, the pumps are located on the pipes $8 \rightarrow 1$, $9 \rightarrow 2$, and $4 \rightarrow 5$.

Pressure-reducing valves: Let R_{ij}^t denote the head loss along a pipe ij with a valve. Then, the following equations pertain to a pipe with a valve in an “on” state:

$$R_{ij}^t = (h_i^t + \bar{h}_i) - (h_j^t + \bar{h}_j) \quad (11)$$

$$q_{ij}^t \geq 0, \quad \forall ij \in \mathcal{V}, \quad \forall t = 1, \dots, T. \quad (12)$$

In Fig. 1, two valves are present on the pipe between the junctions 1 and 2, as well as between junctions 3 and 6.

Pipes without pumps or valves: Nodal pressure heads are related by head losses. The following constraints must be satisfied for pipes without pumps or valves:

$$\tilde{h}_{ij}^t = (h_i^t + \bar{h}_i) - (h_j^t + \bar{h}_j) \quad (13)$$

$$q_{ij}^t \geq 0, \quad \forall ij \in \mathcal{L}/(\mathcal{P} \cup \mathcal{V}), \quad \forall t = 1, \dots, T. \quad (14)$$

The head loss, \tilde{h}_{ij}^t , can be approximated by the following Darcy-Weisbach equation:

$$\tilde{h}_{ij}^t = F_{ij} (q_{ij}^t)^2, \quad \forall ij \in \mathcal{L}/(\mathcal{P} \cup \mathcal{V}), \quad \forall t = 1, \dots, T \quad (15)$$

where the parameter F_{ij} depends on the pipe characteristics.

Power consumption of pumps: Let ρ denote the water density, g the standard gravity coefficient, and η_{ij} the efficiency of pump ij . Then, the power consumption of pump ij at time t is given by the following expression [38]:

$$p_{\text{pump},ij}^t = \frac{\rho g}{\eta_{ij}} \hat{h}_{ij}^t q_{ij}^t \quad (16)$$

for all $t = 1, \dots, T$.

Equation (16) captures a fundamental *coupling* between the water network and the power system because it relates the electrical power consumption of a pump with the volumetric water flow rate and the head gain.

III. MODELING POWER DISTRIBUTION NETWORKS

In this section, we outline the so-called bus injection model for a distribution feeder [32]. The advantage of the bus injection model is that it facilitates the formulation of the AC power flow equations in a (nonconvex) quadratic form [27]. For ease of exposition and notational simplicity, the model is outlined for a balanced system; however, the proposed technical approach naturally extends to unbalanced multiphase systems as shown in [27].

Let $\mathcal{M} = \{0, 1, \dots, M\}$ denote the set of nodes of the power distribution network. Assume that node 0 corresponds to the substation, and define $\mathcal{M}^+ := \mathcal{M} \setminus \{0\}$. Let \mathcal{E} denote the set of distribution lines connecting the nodes. An example of power distribution network is illustrated in Fig. 2; the distribution network is formed by 13 buses and 12 lines; the substation (i.e., the

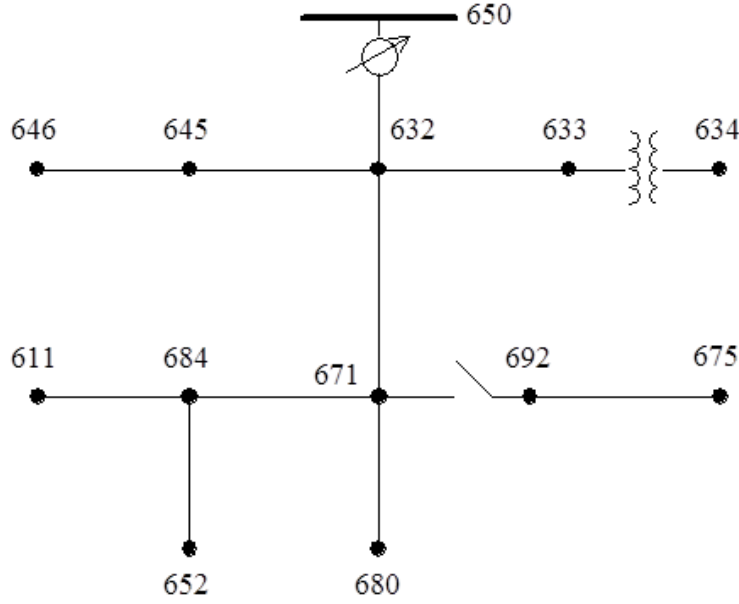


Fig. 2. Example of distribution network: the IEEE 13-node feeder. This feeder will be utilized in the experiments.

point of connection with the transmission grid) is located at node 650. For each node $m \in \mathcal{M}$, let v_m^t denote its complex voltage, and let s_m^t denote the net complex power injection at the same node at time $t = 1, \dots, T$. For each line $(m, n) \in \mathcal{E}$, let z_{mn} and y_{mn} denote the complex series impedance and shunt admittance of a π -equivalent circuit model. The admittance matrix \mathbf{Y} is obtained by setting to $-z_{mn}^{-1}$, $(m, n) \in \mathcal{E}$, its off-diagonal elements, whereas the m -th diagonal element is given by $\sum_{n: (m, n) \in \mathcal{E}} (z_{mn}^{-1} + \frac{1}{2}y_{mn})$. Accordingly, using Ohm's Law and Kirchhoff's Law, the vector of current injections $\mathbf{i}^t := [i_0^t, i_1^t, \dots, i_M^t]^T$ and the vector of voltages $\mathbf{v}^t := [v_0^t, v_1^t, \dots, v_M^t]^T$ are related as:

$$\mathbf{i}^t = \mathbf{Y} \mathbf{v}^t \quad (17)$$

The net complex power injection s_m^t is given by $s_m^t = v_m^t (i_m^t)^*$. Through standard manipulations, the net active and reactive power injections at node m can be expressed as:

$$p_m^t = \mathbf{v}^{tH} \mathbf{Y}_m \mathbf{v}^t \quad (18)$$

$$q_m^t = \mathbf{v}^{tH} \bar{\mathbf{Y}}_m \mathbf{v}^t \quad (19)$$

where the Hermitian matrices \mathbf{Y}_m and $\bar{\mathbf{Y}}_m$ are given by:

$$\mathbf{Y}_m = \frac{1}{2} (\mathbf{e}_m \mathbf{e}_m^T \mathbf{Y} + \mathbf{Y}^H \mathbf{e}_m \mathbf{e}_m^T) \quad (20)$$

$$\bar{\mathbf{Y}}_m = \frac{j}{2}(\mathbf{e}_m \mathbf{e}_m^T \mathbf{Y} - \mathbf{Y}^H \mathbf{e}_m \mathbf{e}_m^T) \quad (21)$$

and \mathbf{e}_m represents the $(m+1)$ -th basis of \mathbb{R}^{M+1} . Similarly, the squared voltage magnitude at node m can be expressed as:

$$|v_m^t|^2 = \mathbf{v}^{tH} \mathbf{M}_m \mathbf{v}^t \quad (22)$$

where $\mathbf{M}_m := \mathbf{e}_m \mathbf{e}_m^T$.

Define $\mathcal{D} \subseteq \mathcal{M}^+$ to be the subset of nodes where controllable DERs are located, and let $p_{r,m}^t$ and $q_{r,m}^t$ denote the active and reactive power generations from the DER(s) at node m at time t . The power setpoints for a DER at node m are assumed to lie within a set:

$$(p_{r,m}^t, q_{r,m}^t) \in \mathcal{C}_m^t \subset \mathbb{R}^2 \quad (23)$$

which is assumed convex. For DERs such as photovoltaic (PV) systems, energy storage systems, and electric vehicles, the set \mathcal{C}_m^t is described by linear inequality constraints or convex quadratic constraints [27], [32], [39]. Let $p_{L,m}^t$ and $q_{L,m}^t$ denote the (noncontrollable) active and reactive loads at node $m \in \mathcal{M}^+$ at time t . Then, the net real and reactive power injections at node $m \in \mathcal{M}^+$ are given by:

$$p_m^t = p_{r,m}^t - p_{L,m}^t, \quad (24)$$

$$q_m^t = q_{r,m}^t - q_{L,m}^t. \quad (25)$$

For any node $m \notin \mathcal{D}$, we have that $p_{r,m}^t = 0$ and $q_{r,m}^t = 0$. For notational simplicity, we assume that one DER is connected at a node of the power system, and we do not describe additional constraints governing the operation of energy storage systems and electric vehicles; however, the methodology proposed in the following sections is straightforwardly applicable to the case where multiple DERs are connected at a node and where the OWPF problem includes the constraints for, e.g., the state of charges of energy storage systems and electric vehicles.

IV. THE OWPF PROBLEM

Water and power networks are coupled because the power consumed by a pump is proportional to the pump's pressure gain times its flow rate. Assume that a pump $ij \in \mathcal{P}$ is electrically connected to one node in the power network. Let $\sigma : \mathcal{P} \rightarrow \mathcal{M}$ map water pumps to the electrical nodes to which they are connected; for example, if pump $ij \in \mathcal{P}$ is connected to node $m \in \mathcal{M}$

of the distribution system, then $m = \sigma(ij)$. For the electrical nodes $\sigma(\mathcal{P})$, we can substitute (16) into (24) to obtain:

$$p_{\sigma(ij)}^t = p_{r,\sigma(ij)}^t - p_{L,\sigma(ij)}^t - \frac{\rho g}{\eta_{ij}} \hat{h}_{ij}^t q_{ij}^t \quad (26)$$

which couples optimization variables in both the water and power networks.

With (26) in place, we formulate OWPF as the following multi-period optimization problem:

$$\min \sum_{t=1}^T \left(C_s^t(\mathbf{v}^t, p_0^t) + \sum_{m \in \mathcal{D}} C_{c,m}^t(p_{r,m}^t, q_{r,m}^t) + \sum_{ij \in \mathcal{P}} C_{w,\sigma(ij)}^t(p_{\sigma(ij)}^t) \right) \quad (27a)$$

$$\text{over } \{\mathbf{v}^t, \{p_{r,m}^t, q_{r,m}^t\}_{\forall m \in \mathcal{D}}\}_{\forall t=1,\dots,T}$$

$$\{q^t, h^t, \hat{h}^t, \tilde{h}^t, w^t, R^t\}_{\forall t=1,\dots,T}$$

$$\text{s.t. } (1)-(15), (18)-(19), (23), (25)$$

$$p_m^t = p_{r,m}^t - p_{L,m}^t - \frac{\rho g}{\eta_{ij}} \hat{h}_{ij}^t q_{ij}^t \quad \forall m \in \sigma(\mathcal{P}) \quad (27b)$$

$$p_m^t = p_{r,m}^t - p_{L,m}^t, \quad \forall m \in \mathcal{M}^+ \setminus \sigma(\mathcal{P}) \quad (27c)$$

$$v_0^t = v_0^{\text{ref}}, \quad \forall t = 1, \dots, T \quad (27d)$$

$$\underline{v}^2 \leq \mathbf{v}^{tH} \mathbf{M}_m \mathbf{v}^t \leq \bar{v}^2, \quad \forall m \in \mathcal{M}^+, \forall t \quad (27e)$$

where the constraint (27d) specifies a constant voltage magnitude v_0^{ref} at the power substation, and (27e) imposes the voltage regulation requirement for the other nodes (i.e., ANSI C84.1 limits). Additional engineering constraints for the power network such as ampacity limits or flow limits can be added without requiring modifications to the procedure outlined in the next section [27].

The cost function (27a) is composed of three terms:

- 1) *Power system operator cost* (C_s^t): this function captures operational objectives of the power network operator; for example, minimization of voltage deviations, minimization of power losses, or deviations from given setpoints for the power at the substation. For example, the latter can be expressed as $c_s(p_0^t - p_{0,\text{set}}^t)^2$, where $c_s > 0$ is a given constant/price.
- 2) *DER cost* ($C_{c,m}^t$): this function captures DER-related objectives. For example, for a PV system, one might consider the cost $\beta^t(\bar{p}_m^t - p_{r,m}^t) + R_c(p_{r,m}^t)$, where \bar{p}_m^t denotes the active power available from a PV system located at node m at time t (based on prevailing irradiance conditions), β^t is the price of power or reward for ancillary service provisioning (received

by the customers from the utility) at time t , and the function $R_c(p_{r,m}^t)$ represents a convex regularization term that can be used to promote solutions with specific characteristics.

- 3) *Water network cost* ($C_{w,\sigma(ij)}^t$): this function models objectives of the water network operator. For example, payments of the water network operator for the power consumed by the pumps can be expressed as $\alpha^t p_{\sigma(ij)}^t + R_w(p_{\sigma(ij)}^t)$, where α^t is the price of electricity (received from the power systems operator) and the regularization term $R_w(p_{\sigma(ij)}^t)$ is used again to promote the preferred features of the optimal solution (e.g., smoothness or sparsity). In particular, the sparsity of the solution leads to the case where only a subset of the pumps are used. On the other hand, the smoothness of the solution prevent the case where one of the pumps is overloaded while the other pumps do not operate.

In the OWPF problem (27), the coupling across multiple time periods appears only in the tank dynamics (3) (with $h_k^{0,\text{out}}$ in (3) a given constant); however, additional constraints for the state of charge of energy storage systems and electric vehicles can be straightforwardly added to the problem formulation.

Problem (27) is *nonconvex* because of the constraints (6), (15), (18), (19), (27b), and the lower bound in (27e); however, these constraints will be reformulated as nonconvex quadratic inequalities in the following section, and they will be efficiently managed by the FPP-SCA approach [26], [27].

V. SUCCESSIVE CONVEX APPROXIMATION

The FPP-SCA is a two-step algorithm that solves convex problems iteratively. In the first step, a feasible solution is obtained by solving an inner approximation of (27). The inner approximation is obtained by rewriting a nonconvex quadratic inequality as a difference of two convex functions, and then linearizing the concave term around a given restriction point. To promote the feasibility of the approximation, we add slack variables to the constraints and minimize the norm of the slack variables over the approximate feasible set. We then use the solution as a restriction point for the next step. If the slack variables become zero, we by construction have a feasible point of (27). In the second stage, we solve a sequence of convex inner approximations of (27) until convergence to a KKT point.

A. Nonconvexity in Power Network Constraints

Notice first that the matrices \mathbf{Y}_m and $\overline{\mathbf{Y}}_m$ are indefinite [32]. Rewrite (18) as the following two inequalities:

$$\mathbf{v}^{tH} \mathbf{Y}_m \mathbf{v}^t \leq p_m^t, \quad (28)$$

$$\mathbf{v}^{tH} (-\mathbf{Y}_m) \mathbf{v}^t \leq -p_m^t. \quad (29)$$

Constraint (28) can be rewritten as:

$$\mathbf{v}^{tH} (\mathbf{Y}_m^{(+)} + \mathbf{Y}_m^{(-)}) \mathbf{v}^t \leq p_m^t \quad (30)$$

where $\mathbf{Y}_m^{(+)}$ and $\mathbf{Y}_m^{(-)}$ are the positive and negative semidefinite parts of matrix \mathbf{Y}_m (obtained through eigenvalue decomposition). Focusing on the negative semidefinite matrix $\mathbf{Y}_m^{(-)}$, we can write:

$$(\mathbf{v}^t - \mathbf{u}^t)^H \mathbf{Y}_m^{(-)} (\mathbf{v}^t - \mathbf{u}^t) \leq 0 \quad (31)$$

where \mathbf{u}^t is a *restriction point*. By rearranging terms, we get:

$$\mathbf{v}^{tH} \mathbf{Y}_m^{(-)} \mathbf{v}^t \leq 2\Re\{\mathbf{u}^{tH} \mathbf{Y}_m^{(-)} \mathbf{v}^t\} - \mathbf{u}^{tH} \mathbf{Y}_m^{(-)} \mathbf{u}^t. \quad (32)$$

Using (32), a convex surrogate of the nonconvex constraint (28) can be obtained as follows:

$$\mathbf{v}^{tH} \mathbf{Y}_m^{(+)} \mathbf{v}^t + 2\Re\{\mathbf{u}^{tH} \mathbf{Y}_m^{(-)} \mathbf{v}^t\} \leq p_m^t + \mathbf{u}^{tH} \mathbf{Y}_m^{(-)} \mathbf{u}^t + s_{m,t}^{(p)} \quad (33)$$

where the non-negative slack variable $s_{m,t}^{(p)}$ is utilized to ensure the feasibility of the constraint. Similarly, the nonconvex constraint (29) is replaced by:

$$-\mathbf{v}^{tH} \mathbf{Y}_m^{(-)} \mathbf{v}^t - 2\Re\{\mathbf{u}^{tH} \mathbf{Y}_m^{(+)} \mathbf{v}^t\} \leq -p_m^t - \mathbf{u}^{tH} \mathbf{Y}_m^{(+)} \mathbf{u}^t + s_{m,t}^{(p)}. \quad (34)$$

Following a similar procedure, the quadratic equality constraint (19) can be replaced by the following convex constraints:

$$\mathbf{v}^{tH} \overline{\mathbf{Y}}_m^{(+)} \mathbf{v}^t + 2\Re\{\mathbf{u}^{tH} \overline{\mathbf{Y}}_m^{(-)} \mathbf{v}^t\} \leq q_m^t + \mathbf{u}^{tH} \overline{\mathbf{Y}}_m^{(-)} \mathbf{u}^t + s_{m,t}^{(q)}, \quad (35)$$

$$-\mathbf{v}^{tH} \overline{\mathbf{Y}}_m^{(-)} \mathbf{v}^t - 2\Re\{\mathbf{u}^{tH} \overline{\mathbf{Y}}_m^{(+)} \mathbf{v}^t\} \leq -q_m^t - \mathbf{u}^{tH} \overline{\mathbf{Y}}_m^{(+)} \mathbf{u}^t + s_{m,t}^{(q)} \quad (36)$$

where the $s_{m,t}^{(q)}$ is added in order to ensure feasibility of the convex inner-approximation, while $\overline{\mathbf{Y}}_m^{(+)}$ and $\overline{\mathbf{Y}}_m^{(-)}$ are the positive and negative semidefinite parts of $\overline{\mathbf{Y}}_m$.

Finally, the lower bound on the bus voltage magnitude (27e) is replaced by:

$$-2\Re\{\mathbf{u}^{tH} \mathbf{M}_m \mathbf{v}^t\} \leq -\underline{v}^2 - \mathbf{u}^{tH} \mathbf{M}_m \mathbf{u}^t + s_{m,t}^{(v)}, \quad (37)$$

where $s_{m,t}^{(v)}$ is a non-negative slack variable.

B. Nonconvexity in Water Network Constraints

Constraint (6) is nonconvex. However, it has been shown in [18] that (6) can be replaced by the following constraint without loss of optimality:

$$\hat{h}_{ij}^t \leq A_{ij} (q_{ij}^t)^2 + B_{ij}^{\max} q_{ij}^t + C_{ij}^{\max}, \quad (38)$$

where $B_{ij}^{\max} := B_{ij} w_{ij}^{\max}$ and $C_{ij}^{\max} := C_{ij} (w_{ij}^{\max})^2$. Because $A_{ij} < 0$, (38) is a convex quadratic constraint. With this reformulation, the variables w_{ij}^t can be eliminated; in fact, a unique w_{ij}^t that satisfies (7) can always be recovered from any feasible solution $(q_{ij}^t, \hat{h}_{ij}^t)$.

Next, consider replacing (15) with the following two inequalities:

$$\tilde{h}_{ij}^t \geq F_{ij} (q_{ij}^t)^2 \quad (39)$$

$$-\tilde{h}_{ij}^t \geq -F_{ij} (q_{ij}^t)^2 \quad (40)$$

and notice that (39) is convex because $F_{ij} > 0$ [18]. On the other hand, (40) is nonconvex. A convex restriction of (40) can be written as:

$$F_{ij} (z_{q,ij}^t)^2 - 2z_{q,ij}^t F_{ij} q_{ij}^t \leq -\tilde{h}_{ij}^t + s_{ij,t}^{(q)} \quad (41)$$

where the non-negative slack variable $s_{ij,t}^{(q)}$ is added to insure feasibility.

Regarding the power balance constraint (27b), it is convenient to introduce the auxiliary variables β_{ij}^t and $p_{\text{pump},ij}^t$ per pump $ij \in \mathcal{P}$, and rewrite (27b) as the following equivalent set of constraints:

$$p_{\sigma(ij)}^t = p_{r,\sigma(ij)}^t - p_{L,\sigma(ij)}^t - p_{\text{pump},\sigma(ij)}^t \quad (42)$$

$$\beta_{ij}^t = p_{\text{pump},ij}^t \quad (43)$$

$$\beta_{ij}^t = \frac{\rho g}{\eta_{ij}} \hat{h}_{ij}^t q_{ij}^t. \quad (44)$$

The auxiliary variables β_{ij}^t and $p_{\text{pump},ij}^t$ facilitate the application of the FPP-SCA method as well as the development of a distributed algorithm in Section VI. Re-express (44) as:

$$\mathbf{y}_{ij}^t{}^T \mathbf{T}_{ij} \mathbf{y}_{ij}^t \leq -\beta_{ij}^t \quad (45)$$

$$\mathbf{y}_{ij}^t{}^T (-\mathbf{T}_{ij}) \mathbf{y}_{ij}^t \leq \beta_{ij}^t \quad (46)$$

where $\mathbf{y}_{ij}^t := [\hat{h}_{ij}^t, q_{ij}^t]^T$ for simplicity and \mathbf{T}_{ij} is a two-by-two matrix with $\frac{\rho g}{2\eta_{ij}}$ on the off-diagonal entries. Constraints (45)–(46) are nonconvex. Rewriting \mathbf{T}_{ij} as $\mathbf{T}_{ij} = \mathbf{T}_{ij}^{(+)} + \mathbf{T}_{ij}^{(-)}$,

where $\mathbf{T}_{ij}^{(+)}$ and $\mathbf{T}_{ij}^{(-)}$ are the positive and negative semidefinite parts of \mathbf{T}_{ij} , surrogate convex constraints for (45) and (46) can be written as:

$$\mathbf{y}_{ij}^t T \mathbf{T}_{ij}^{(+)} \mathbf{y}_{ij}^t + 2\mathbf{z}_{ij}^t T \mathbf{T}_{ij}^{(-)} \mathbf{y}_{ij}^t \leq -\beta_{ij}^t + \mathbf{z}_{ij}^t T \mathbf{T}_{ij}^{(-)} \mathbf{z}_{ij}^t + s_{ij,t}^{(p)}, \quad (47)$$

$$-\mathbf{y}_{ij}^t T \mathbf{T}_{ij}^{(-)} \mathbf{y}_{ij}^t - 2\mathbf{z}_{ij}^t T \mathbf{T}_{ij}^{(+)} \mathbf{y}_{ij}^t \leq \beta_{ij}^t - \mathbf{z}_{ij}^t T \mathbf{T}_{ij}^{(+)} \mathbf{z}_{ij}^t + s_{ij,t}^{(p)} \quad (48)$$

where \mathbf{z}_{ij}^t represents any linearization (restriction) point, and $s_{ij,t}^{(p)}$ is a non-negative slack variable.

We are now ready to outline the FPP-SCA algorithm for solving OWPF – the subject of the next section.

C. FPP-SCA Algorithm

For notational simplicity, collect in the matrices $\mathbf{S}_p, \mathbf{S}_q, \mathbf{S}_v \in \mathbb{R}_+^{M \times T}$ the slack variables $s_{m,t}^{(p)}$, $s_{m,t}^{(q)}$, and $s_{m,t}^{(v)}$, respectively. Similarly, let the matrices $\bar{\mathbf{S}}_p \in \mathbb{R}_+^{|\mathcal{P}| \times T}$ and $\bar{\mathbf{S}}_q \in \mathbb{R}_+^{n \times T}$, where $n = |\mathcal{L}/(\mathcal{P} \cup \mathcal{V})|$, collect all the slack variables $s_{ij,t}^{(p)}$ and $s_{ij,t}^{(q)}$, respectively. In addition, let $\mathbf{Q}^t \in \mathbb{R}_+^{|\mathcal{L}|}$, $\boldsymbol{\beta}^t \in \mathbb{R}^{|\mathcal{P}|}$, and $\mathbf{h}^t \in \mathbb{R}^{|\mathcal{M}|}$ collect all the water flow variables, powers consumed by pumps, and head pressures. Lastly, let the matrices $\mathbf{Z} \in \mathbb{R}^{2|\mathcal{P}| \times T}$, $\mathbf{Z}_q \in \mathbb{R}^{n \times T}$, and $\mathbf{U} \in \mathbb{C}^{M \times T}$ collect the restriction points \mathbf{z}_{ij}^t , $\mathbf{z}_{q,ij}^t$, and \mathbf{u}^t , respectively.

With this notation in place, define the convex sets $\Psi_{\mathbf{U}}$ and $\Omega_{\mathbf{Z}, \mathbf{Z}_q}$ (which are functions of the restriction points) pertaining to power and water networks, respectively, as:

$$\Psi_{\mathbf{U}} := \left\{ (\{\mathbf{v}^t, \mathbf{p}_r^t, \mathbf{q}_r^t, \mathbf{p}_{\text{pump}}^t\}_{t=1}^T, \mathbf{S}_p, \mathbf{S}_q, \mathbf{S}_v) \mid \begin{array}{l} (23), (25), (27c), (27d), (33)–(37), (42) \\ \mathbf{v}^{tH} \mathbf{M}_m \mathbf{v}^t \leq \bar{v}^2 \quad \forall m \in \mathcal{M}^+, \forall t = 1, \dots, T \end{array} \right\}, \quad (49)$$

$$\Omega_{\mathbf{Z}, \mathbf{Z}_q} := \left\{ (\{\mathbf{Q}^t, \mathbf{h}^t, \boldsymbol{\beta}^t\}_{t=1}^T, \bar{\mathbf{S}}_p, \bar{\mathbf{S}}_q) \mid (1)–(5), (8)–(14), (39), (41), (47), (48) \right\} \quad (50)$$

where $\mathbf{p}_r^t := [\{p_{r,m}^t\}_{m \in \mathcal{D}}]^T$, $\mathbf{q}_r^t := [\{q_{r,m}^t\}_{m \in \mathcal{D}}]^T$, and $\mathbf{p}_{\text{pump}}^t := [\{p_{\text{pump},m}^t\}_{m \in \sigma(\mathcal{P})}]^T$.

It follows that the convex optimization problem to be solved at the k -th iteration of the feasibility phase of the FPP-SCA algorithm can be compactly written as:

$$\begin{aligned} \min \quad & \|\mathbf{S}_p\|_F^2 + \|\mathbf{S}_q\|_F^2 + \|\mathbf{S}_v\|_F^2 + \|\bar{\mathbf{S}}_p\|_F^2 + \|\bar{\mathbf{S}}_q\|_F^2 \\ \text{over} \quad & \{\mathbf{v}^t, \mathbf{p}_r^t, \mathbf{q}_r^t, \mathbf{p}_{\text{pump}}^t\}_{t=1}^T, \mathbf{S}_p, \mathbf{S}_q, \mathbf{S}_v \end{aligned} \quad (51a)$$

$$\begin{aligned} & \{\mathbf{Q}^t, \mathbf{h}^t, \boldsymbol{\beta}^t\}_{t=1}^T, \bar{\mathbf{S}}_p, \bar{\mathbf{S}}_q \\ \text{s.t.} \quad & (\{\mathbf{v}^t, \mathbf{p}_r^t, \mathbf{q}_r^t, \mathbf{p}_{\text{pump}}^t\}_{t=1}^T, \mathbf{S}_p, \mathbf{S}_q, \mathbf{S}_v) \in \Psi_{\mathbf{U}(k)} \end{aligned} \quad (51b)$$

$$\begin{aligned} & (\{\mathbf{Q}^t, \mathbf{h}^t, \boldsymbol{\beta}^t\}_{t=1}^T, \bar{\mathbf{S}}_p, \bar{\mathbf{S}}_q) \in \Omega_{\mathbf{Z}(k), \mathbf{Z}_q(k)} \\ & \beta_{ij}^t = p_{\text{pump}, \sigma(ij)}^t \quad \forall ij \in \mathcal{P}, t = 1, \dots, T \end{aligned} \quad (51c)$$

where the cost function aims to minimize the violation of the nonconvex constraint in the original OWPF, and $\mathbf{U}(k)$, $\mathbf{Z}(k)$, $\mathbf{Z}_q(k)$ are the restriction points at iteration k . In particular, $\mathbf{U}(k)$, $\mathbf{Z}(k)$, $\mathbf{Z}_q(k)$ coincide with the optimal solution of (51) at the previous iteration $k - 1$. Algorithm 1 summarizes the overall feasibility procedure. Notice that problem (51) is a second-order cone program, and observe that the cost function is monotonically nonincreasing because the restriction points are always feasible. Although this method is not guaranteed to find a feasible point, it converged in all simulations to operating points that were feasible for the water and power systems considered.

Algorithm 1: FPP Method for OWPF

Initialization: set $k = 0$ and $\mathbf{U}(0)$ to be all ones, and $\mathbf{Z}(0)$, $\mathbf{Z}_q(0)$ to be all zeros.

repeat

[S1] Solve (51):

$\{\{\mathbf{v}^t(k), \mathbf{p}_r^t(k), \mathbf{q}_r^t(k), \mathbf{p}_{\text{pump}}^t(k)\}_{t=1}^T, \{\mathbf{Q}^t(k), \mathbf{h}^t(k), \boldsymbol{\beta}^t(k)\}_{t=1}^T, \mathbf{S}_p(k), \mathbf{S}_q(k), \mathbf{S}_v(k), \bar{\mathbf{S}}_p(k), \bar{\mathbf{S}}_q(k) \leftarrow$
solution of (51)

[S2] Update restriction points:

$\mathbf{U}(k+1) \leftarrow \{\mathbf{v}^t(k)\}_{t=1}^T$

$\mathbf{Z}(k+1) \leftarrow \{q_{ij}^t(k), \hat{h}_{ij}^t(k), ij \in \mathcal{P}\}_{t=1}^T$

$\mathbf{Z}_q(k+1) \leftarrow \{q_{ij}^t(k), ij \in \mathcal{L}/(\mathcal{P} \cup \mathcal{V})\}_{t=1}^T$

[S3] Increase iteration index:

$k \leftarrow k + 1$.

until $(\|\mathbf{S}_p\|_F^2 + \|\mathbf{S}_q\|_F^2 + \|\mathbf{S}_v\|_F^2 + \|\bar{\mathbf{S}}_p\|_F^2 + \|\bar{\mathbf{S}}_q\|_F^2) \leq \epsilon$

Once a feasible operating point is identified through Algorithm 1, the nonconvex feasible set of OWPF is replaced at each iteration by an inner convex approximation. The optimization problem to be solved at the k -th iteration of the refinement phase can be formulated as:

$$\min \sum_{t=1}^T \left(C_s^t(\mathbf{v}^t, p_0^t) + \sum_{m \in \mathcal{D}} C_{c,m}^t(p_{r,m}^t, q_{r,m}^t) + \sum_{ij \in \mathcal{P}} C_{w,\sigma(ij)}^t(p_{\sigma(ij)}^t) \right) \quad (52a)$$

$$\begin{aligned} \text{over } & \{\mathbf{v}^t, \mathbf{p}_r^t, \mathbf{q}_r^t, \mathbf{p}_{\text{pump}}^t, \mathbf{Q}^t, \mathbf{h}^t, \boldsymbol{\beta}^t\}_{t=1}^T \\ \text{s.t. } & (\{\mathbf{v}^t, \mathbf{p}_r^t, \mathbf{q}_r^t, \mathbf{p}_{\text{pump}}^t\}_{t=1}^T) \in \tilde{\Psi}_{\mathbf{U}(k)} \end{aligned} \quad (52b)$$

$$\begin{aligned} & (\{\mathbf{Q}^t, \mathbf{h}^t, \boldsymbol{\beta}^t\}_{t=1}^T) \in \tilde{\Omega}_{\mathbf{Z}(k), \mathbf{Z}_q(k)} \\ & \beta_{ij}^t = p_{\text{pump}, \sigma(ij)}^t \quad \forall ij \in \mathcal{P}, t = 1, \dots, T \end{aligned} \quad (52c)$$

where $\tilde{\Psi}_{\mathbf{U}(k)}$ is the restriction of the set $\Psi_{\mathbf{U}(k)}$ to the plane $\mathbf{S}_p = \mathbf{S}_q = \mathbf{S}_v = \mathbf{0}$. Similarly, the set $\tilde{\Omega}_{\mathbf{Z}(k), \mathbf{Z}_q(k)}$ is the projection of $\Omega_{\mathbf{Z}(k), \mathbf{Z}_q(k)}$ when $\bar{\mathbf{S}}_q = \bar{\mathbf{S}}_p = \mathbf{0}$. At each step $k = 2, \dots$, the sets $\tilde{\Psi}_{\mathbf{U}(k)}$ and $\tilde{\Omega}_{\mathbf{Z}(k), \mathbf{Z}_q(k)}$ are formed based on the optimal solution of (52) at the previous iteration $k-1$. The proposed methodology generates a monotone sequence that converges to a KKT point of the original OWPF (27), and it is given as Algorithm 2.

Algorithm 2: SCA Method for OWPF

Initialization: set $k = 0$ and construct $\mathbf{U}(0), \mathbf{Z}(0), \mathbf{Z}_q(0)$ based on the solution of Algorithm 1.

repeat

[S1] Solve (52):

$\{\{\mathbf{v}^t(k), \mathbf{p}_r^t(k), \mathbf{q}_r^t(k), \mathbf{p}_{\text{pump}}^t(k)\}_{t=1}^T, \{\mathbf{Q}^t(k), \mathbf{h}^t(k), \boldsymbol{\beta}^t(k)\}_{t=1}^T\} \leftarrow$ solution of (52)

[S2] Update restriction points:

$\mathbf{U}(k+1) \leftarrow \{\mathbf{v}^t(k)\}_{t=1}^T$

$\mathbf{Z}(k+1) \leftarrow \{q_{ij}^t(k), \hat{h}_{ij}^t(k), ij \in \mathcal{P}\}_{t=1}^T$

$\mathbf{Z}_q(k+1) \leftarrow \{q_{ij}^t(k), ij \in \mathcal{L}/(\mathcal{P} \cup \mathcal{V})\}_{t=1}^T$

[S3] Increase iteration index:

$k \leftarrow k + 1.$

until Cost reduction $\leq \epsilon$

Algorithm 2 has converged if the cost function between two consecutive steps is less than a given quantity $0 < \epsilon \ll 1$.

Claim 1 (Convergence). *From [40, Theorem 1], it follows that every limit point generated by the proposed algorithms is a KKT point. Hence, the first phase converges to a KKT point of (51). In addition, if the algorithm starts the second phase from a feasible point, then the sequence converges to the set containing all the KKT points of the problem (27).*

The convergence of the first phase of the algorithm follows from [40]. Since the SCA phase is initialized from a feasible point of the OWPF, the sequence produced by Algorithm 2 is always

feasible; i.e., every point in the sequence lies in the feasibility set of (27). Thus, the sequence converges to a set that contains all the KKT points of (27).

In the next section, a distributed solution strategy will be outlined based on the ADMM.

VI. DISTRIBUTED ALGORITHM

Power and water networks are usually planned and operated independently. In this section, we develop a distributed solver where water and power operators pursue individual operational objectives and retain controllability of their own assets (pumps for the water network and DERs for the power network). In particular, in the proposed setting, each system operator solves a smaller optimization problem with variables associated only with its network and controllable devices – a rendition of the AC optimal power flow for the power network operator, and an optimal water flow problem for the water system operator. The two operators subsequently exchange information regarding the shared variables to *reach consensus* on the powers consumed by the water pumps. Using this approach, both systems keep their private information and only exchange the optimized values of the powers consumed by the pumps.

Assume that each system has determined an operational profile that satisfies all network-level constraints. The proposed technical approach consists of defining the following augmented Lagrangian associated with (52):

$$L_\rho(\{\mathbf{v}^t, \mathbf{p}_r^t, \mathbf{q}_r^t, \mathbf{p}_{\text{pump}}^t, \mathbf{Q}^t, \mathbf{h}^t, \boldsymbol{\beta}^t, \{\nu_{ij}^t\}_{ij \in \mathcal{P}}\}_{t=1}^T) = \sum_{t=1}^T \left(C_s^t(p_0^t) + \sum_{m \in \mathcal{D}} C_{c,m}^t(p_m^t) + \sum_{ij \in \mathcal{P}} C_{w,\sigma(ij)}^t(\beta_{ij}^t) \right. \\ \left. + \sum_{ij \in \mathcal{P}} \nu_{ij}^t (\beta_{ij}^t - p_{\text{pump},\sigma(ij)}^t) + \frac{\rho}{2} (\beta_{ij}^t - p_{\text{pump},\sigma(ij)}^t)^2 \right) \quad (53)$$

where ν_{ij}^t is the dual variable associated with the consensus-enforcing constraint (52c) and $\rho > 0$ is an given parameter.

Leveraging the decomposability of (53), the proposed ADMM-based algorithm is summarized in Algorithm 3, wherein k is the iteration index.

Each iteration of the procedure described in Algorithm 3 consists of two main steps. In step [S1] power and water operators solve two local subproblems to update variables $\{\mathbf{v}^t(k+1), \mathbf{p}_r^t(k+1), \mathbf{q}_r^t(k+1), \mathbf{p}_{\text{pump}}^t(k+1)\}_{t=1}^T$ and $\{\mathbf{Q}^t(k+1), \mathbf{h}^t(k+1), \boldsymbol{\beta}^t(k+1)\}_{t=1}^T$, respectively. The subproblem solved by the power network operator coincides with an AC optimal power flow, with

Algorithm 3: Distributed OWPF algorithm.

Initialization: set $k = 0$, $\nu_{ij}^{t(0)} = 0 \forall ij \in \mathcal{P}, t = 1, \dots, T$, and each system initializes its own variable from a feasible operational profile.

repeat

[S1a] Update power-related variables:

$$(\{\mathbf{v}^t(k+1), \mathbf{p}_r^t(k+1), \mathbf{q}_r^t(k+1), \mathbf{p}_{\text{pump}}^t(k+1)\}_{t=1}^T) \leftarrow \arg \min_{\{\mathbf{v}^t, \mathbf{p}_r^t, \mathbf{q}_r^t, \mathbf{p}_{\text{pump}}^t\} \in \tilde{\Psi}_{\mathbf{U}(k)}} L_\rho(\{\mathbf{v}^t, \mathbf{p}_r^t, \mathbf{q}_r^t, \mathbf{p}_{\text{pump}}^t, \{\nu_{ij}^t(k)\}_{t=1}^T\})$$

[S1b] Update water-related variables:

$$(\{\mathbf{Q}^t(k+1), \mathbf{h}^t(k+1), \boldsymbol{\beta}^t(k+1)\}_{t=1}^T) \leftarrow \arg \min_{(\{\mathbf{Q}^t, \mathbf{h}^t, \boldsymbol{\beta}^t\}_{t=1}^T) \in \tilde{\Omega}_{\mathbf{Z}(k), \mathbf{Z}_q(k)}} L_\rho(\{\{\nu_{ij}^t(k)\}, \mathbf{Q}^t, \mathbf{h}^t, \boldsymbol{\beta}^t\}_{t=1}^T)$$

[S2] Update dual variables:

for $ij \in \mathcal{P}, t = 1, \dots, T$ **do**

$\nu_{ij}^t(k+1) = \nu_{ij}^t(k) + \rho(\beta_{ij}^t(k+1) - p_{\text{pump}, \sigma(ij)}^t(k+1))$

end

[S3] Update restriction points:

$\mathbf{U}(k+1) \leftarrow \{\mathbf{v}^t(k+1)\}_{t=1}^T$

$\mathbf{Z}(k+1) \leftarrow \{q_{ij}^t(k+1), \hat{h}_{ij}^t(k+1), ij \in \mathcal{P}\}_{t=1}^T$

$\mathbf{Z}_q(k+1) \leftarrow \{q_{ij}^t(k+1), ij \in \mathcal{L}/(\mathcal{P} \cup \mathcal{V})\}_{t=1}^T$

[S4] Increase iteration index: $k \leftarrow k + 1$

until convergence criterion is met

the cost augmented by the consensus-enforcing regularization term $\sum_{t=1}^T \sum_{m \in \sigma(\mathcal{P})} (-\nu_m^t p_{\text{pump}, m}^t + \frac{\rho}{2} (\beta_m^t(k) - p_{\text{pump}, m}^t)^2)$. The problem solved by the water system operator is an optimal water flow [18], augmented with the regularization term $\sum_{t=1}^T \sum_{ij \in \mathcal{P}} (\nu_{ij}^t \beta_{ij}^t + \frac{\rho}{2} (\beta_{ij}^t - p_{\text{pump}, \sigma(ij)}^t(k))^2)$. After solving the two problems, the water and power operators exchange the variables $\{p_{\text{pump}, m}^t(k+1)\}$ and $\{\beta_m^t(k+1)\}$ and they locally perform the dual step in [S2]. The algorithm terminates when the norm of the difference between two consecutive restriction points is less than ϵ . Once the algorithm terminates, it holds that $\beta_{ij}^t = p_{\text{pump}, \sigma(ij)}^t$; i.e., the two systems agree on the power consumed by the pumps.

VII. EXPERIMENTAL RESULTS

In this section, the proposed approach is tested in a setting where the IEEE 13-node test feeder is coupled with a municipal water distribution network [36]. The OWPF is solved using the proposed centralized and the distributed solvers. The MATLAB-based optimization package

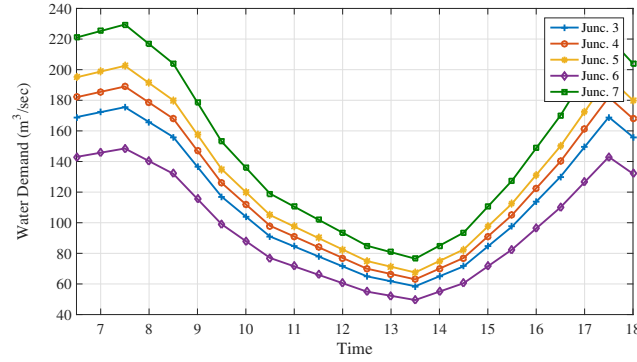


Fig. 3. Water demand at the junctions with time

YALMIP [41] is used along with the interior-point solver SeDuMi [42]. The centralized solver initializes the voltage with the flat voltage profile; the parameter ϵ is set to 10^{-5} .

The water network is shown in Fig. 1 and it is modified version of the ones described in [36]. It consists of 7 junctions, 2 reservoirs, and a tank and it features 5 pipes, 2 pressure-reducing valves, and 3 pumps. The elevation of all junctions and the minimum allowable head pressure are given in Table I. The elevation of the water reservoirs at nodes 8 and 9 are -2.5 meters and 5 meters, respectively. The water demands over the optimization time at junctions 3, 4, 5, 6, and 7 are shown in Fig. 3. The tank has an area of 490.87 m^2 and maximum height of 30 meters. The initial height of the water in the tank is 10 meters. As an example of application, the optimization problem is solved over an interval of 12 hours (from 6 AM to 6 PM), with intervals of 30 minutes. The regularization term of the water cost function is chosen to be the Frobenius norm of the power consumption of the pumps over the optimization period with a weight of 10^{-3} .

The pumping stations are connected to the IEEE 13-node distribution test feeder, which is shown in Fig. 2. In particular, pump $8 \rightarrow 1$ is connected to node 633 of the feeder, pump $9 \rightarrow 2$ to node 645, and pump $4 \rightarrow 5$ to node 684. A single-phase model of the distribution feeder is considered, wherein PV inverters are assumed to be located at the nodes 634, 646, 675, 611, and 652. Because of the high PV penetration, the system is likely to experience overvoltage challenges. In this case, curtailment of the active power at the PV units is necessary to maintain voltage magnitudes within prescribed limits. The prices of electricity (utilized in the cost function for the water network and to discourage curtailment from PV systems) are obtained from the

TABLE I
JUNCTIONS DETAILS.

Junction	Elevation (m)	Minimum Head Pressure (m)
1	6	0
2	33	0
3	1.5	35
4	-8	40
5	33	40
6	8	35
7	4	40

Midcontinent Independent System Operator¹ for June, 20, 2017. The regularization term of the curtailment cost function is chosen to be a weighted Frobenius norm of the active power curtailed during the optimization period with a weight of 10^{-3} .

The OWPF strategy is compared to the decoupled case, where: 1) water system operator solves an optimal flow problem to minimize the power consumption based on the electricity prices [18]; 2) the powers consumed by the water pumps are then used as inputs to the AC optimal power flow problem (i.e., they are uncontrollable loads) solved by the power distribution operator, where the power curtailment from the V systems is minimized along with the discrepancy from a given setpoint for the power at the substation [35]. Table II summarizes the achieved costs in the two cases. The total cost across the two systems is significantly lower in the OWPF case. It is clear that a coupled optimization approach enhances flexibility, which reduces the total cost compared to the decoupled optimization strategy. The operating cost of the water system is increased, and an increased amount of water in the tank at the end of the 12-hour optimization slot is observed; this calls for a systematic payment to the water system operator for providing services – an interesting future research topic. On the other hand, the cost of PV power curtailment is almost halved, thus enabling a significantly higher utilization of renewable-based power. Fig. 4 illustrates the power profiles using OWPF, while Fig. 5 shows the same profiles for the decoupled approach.

Finally, the convergence characteristics of the proposed distributed algorithms are demonstrated

¹Available at: <https://www.misoenergy.org>

TABLE II
RESULTS OF OWPF FORMULATION AND THE DECOUPLED APPROACH.

Cost	OWPF	Decoupled Solver
Water Cost	460.26	268.47
Curtailement Cost	769.30	1506.17
Substation Cost	170.11	23.94
Total Cost	1399.67	1798.58

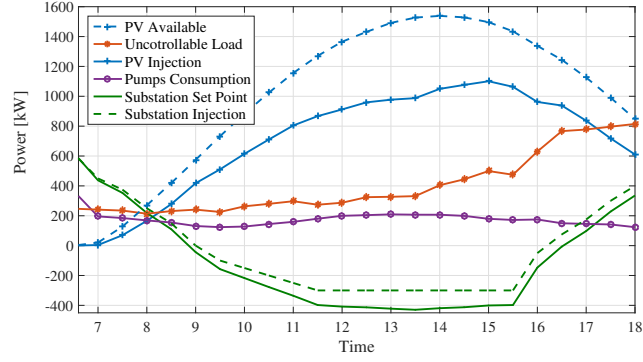


Fig. 4. OWPF approach solution.

using the same power and water networks. Each network operator initializes its local variables by optimizing a local operational cost without considering the other network constraints (i.e., the decoupled solution). Then, the distributed algorithm is used to reach a consensus on the powers consumed by the water pumps. The value of the parameter ρ is chosen to be 10^6 . Fig. 6 shows the cost of operating the pumps at each local solver per each iteration. The discrepancy between the variables β_{ij}^t and $p_{\sigma(ij)}^t$ is shown in Fig. 7 by considering the Frobenius norm square measure of the difference between the two quantities in per unit. After approximately 50 iterations, the consensus error is lower than 1%.

VIII. CONCLUSIONS

This paper presented an OWPF problem to optimize the use of controllable assets across power and water systems while accounting for the couplings between the two infrastructures. Although the physics governing the operation of the two systems and coupling constraints lead to a nonconvex problem, feasible point pursuit-successive convex approximation approach was

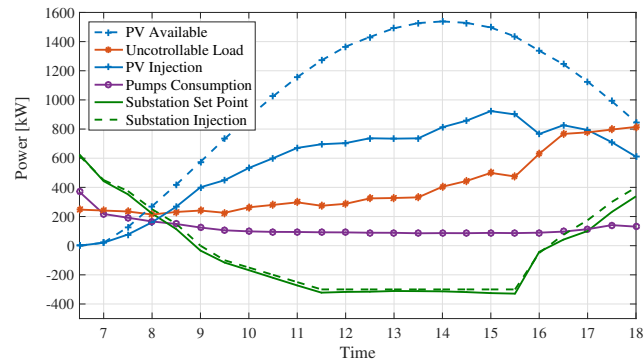


Fig. 5. Decoupled approach solution.

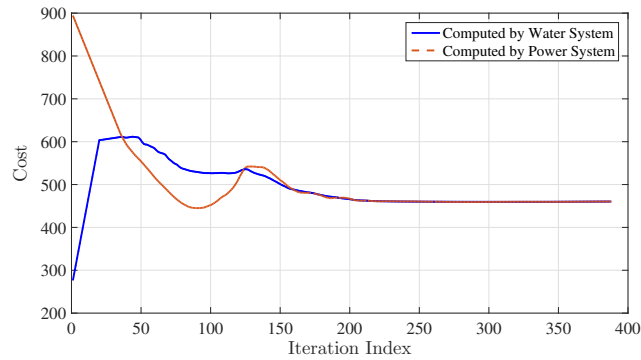


Fig. 6. Operational cost of the water network by each system.

proposed to identify feasible and optimal solutions. A distributed solver based on the ADMM was developed to enable water and power operators to pursue individual objectives while respecting the couplings between the two networks. The merits of the proposed approach were demonstrated for the case of a distribution feeder coupled with a municipal water distribution network. Future efforts will look at incorporating pump selection strategies into the OWPF, as well as the formulation of stochastic OWPF problems to account for errors in the forecasts of power and water demands as well as powers available from renewable-based distributed energy resources.

REFERENCES

- [1] M. H. Albadi and E. El-Saadany, "A summary of demand response in electricity markets," *Electric power systems research*, vol. 78, no. 11, pp. 1989–1996, 2008.

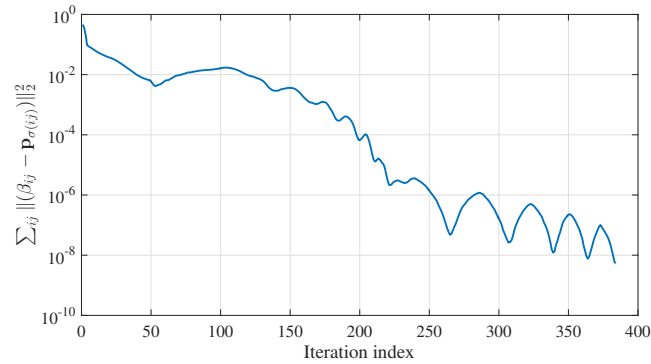


Fig. 7. Convergence of the distributed solver.

- [2] P. Siano, “Demand response and smart grid—a survey,” *Renewable and Sustainable Energy Reviews*, vol. 30, pp. 461–478, 2014.
- [3] G. Marks, E. Wilcox, D. Olsen, and S. Goli, “Opportunities for demand response in California agricultural irrigation – a scoping study,” iP Solutions Corp. and Lawrence Berkeley National Laboratory, Tech. Rep., 2013.
- [4] E. A. Byers, J. W. Hall, and J. M. Amezcaga, “Electricity generation and cooling water use: UK pathways to 2050,” *Global Environmental Change*, vol. 25, pp. 16–30, 2014.
- [5] J. Colman, “The effect of ambient air and water temperature on power plant efficiency,” *Duke University Libraries*, 2013.
- [6] B. Wang, Y. Zhou, P. Mancarella, and M. Panteli, “Assessing the impacts of extreme temperatures and water availability on the resilience of the GB power system,” in *Power System Technology, 2016 IEEE International Conference on*. IEEE, 2016, pp. 1–6.
- [7] D. Denig-Chakroff, “Reducing electricity used for water production: Questions state commissions should ask regulated utilities,” *Water Research and Policy*, 2008.
- [8] P. W. Jowitt and G. Germanopoulos, “Optimal pump scheduling in water-supply networks,” *Journal of Water Resources Planning and Management*, vol. 118, no. 4, pp. 406–422, 1992.
- [9] C. Giacomello, Z. Kapelan, and M. Nicolini, “Fast hybrid optimization method for effective pump scheduling,” *Journal of Water Resources Planning and Management*, vol. 139, no. 2, pp. 175–183, 2012.
- [10] D. Verleye and E.-H. Aghezzaf, “Optimising production and distribution operations in large water supply networks: A piecewise linear optimisation approach,” *International Journal of Production Research*, vol. 51, no. 23-24, pp. 7170–7189, 2013.
- [11] H. D. Sherali, S. Subramanian, and G. Loganathan, “Effective relaxations and partitioning schemes for solving water distribution network design problems to global optimality,” *Journal of Global Optimization*, vol. 19, no. 1, pp. 1–26, 2001.
- [12] J. Burgschweiger, B. Gnädig, and M. C. Steinbach, “Optimization models for operative planning in drinking water networks,” *Optimization and Engineering*, vol. 10, no. 1, pp. 43–73, 2009.
- [13] B. Ulanicki, J. Kahler, and H. See, “Dynamic optimization approach for solving an optimal scheduling problem in water distribution systems,” *Journal of Water Resources Planning and Management*, vol. 133, no. 1, pp. 23–32, 2007.
- [14] L. M. Brion and L. W. Mays, “Methodology for optimal operation of pumping stations in water distribution systems,” *Journal of Hydraulic Engineering*, vol. 117, no. 11, pp. 1551–1569, 1991.

- [15] B. Ghaddar, J. Naoum-Sawaya, A. Kishimoto, N. Taheri, and B. Eck, "A Lagrangian decomposition approach for the pump scheduling problem in water networks," *European Journal of Operational Research*, vol. 241, no. 2, pp. 490–501, 2015.
- [16] G. Yu, R. Powell, and M. Sterling, "Optimized pump scheduling in water distribution systems," *Journal of Optimization Theory and Applications*, vol. 83, no. 3, pp. 463–488, 1994.
- [17] A. Gleixner, H. Held, W. Huang, and S. Vigerske, "Towards globally optimal operation of water supply networks," *Numerical Algebra, Control and Optimization*, vol. 2, no. 4, pp. 695–711, 2012.
- [18] D. Fooladivanda and J. A. Taylor, "Energy-optimal pump scheduling and water flow," *IEEE Transactions on Control of Network Systems*, 2017.
- [19] K. Oikonomou, M. Parvania, and S. Burian, "Integrating water distribution energy flexibility in power systems operation," in *IEEE Power & Energy Society General Meeting*, 2017.
- [20] B. Barán, C. von Lücken, and A. Sotelo, "Multi-objective pump scheduling optimisation using evolutionary strategies," *Advances in Engineering Software*, vol. 36, no. 1, pp. 39–47, 2005.
- [21] J.-Y. Wang, T.-P. Chang, and J.-S. Chen, "An enhanced genetic algorithm for bi-objective pump scheduling in water supply," *Expert Systems with Applications*, vol. 36, no. 7, pp. 10 249–10 258, 2009.
- [22] U. Zessler and U. Shamir, "Optimal operation of water distribution systems," *Journal of water resources planning and management*, vol. 115, no. 6, pp. 735–752, 1989.
- [23] V. Nitivattananon, E. C. Sadowski, and R. G. Quimpo, "Optimization of water supply system operation," *Journal of Water Resources Planning and Management*, vol. 122, no. 5, pp. 374–384, 1996.
- [24] K. E. Lansey and K. Awu, "Optimal pump operations considering pump switches," *Journal of Water Resources Planning and Management*, vol. 120, no. 1, pp. 17–35, 1994.
- [25] E. Dall'Anese, P. Mancarella, and A. Monti, "Unlocking flexibility: Integrated optimization and control of multi-energy systems," *IEEE Power and Energy Magazine*, vol. 15, no. 1, pp. 43–52, Jan 2017.
- [26] O. Mehanna, K. Huang, B. Gopalakrishnan, A. Konar, and N. D. Sidiropoulos, "Feasible point pursuit and successive approximation of non-convex QCQPs," *IEEE Signal Processing Letters*, vol. 22, no. 7, pp. 804–808, 2015.
- [27] A. S. Zamzam, N. D. Sidiropoulos, and E. Dall'Anese, "Beyond relaxation and newton-raphson: Solving AC OPF for multi-phase systems with renewables," *IEEE Trans. on Smart Grid*, July 2017.
- [28] S. Boyd, N. Parikh, E. Chu, B. Peleato, and J. Eckstein, "Distributed optimization and statistical learning via the alternating direction method of multipliers," *Foundations and Trends® in Machine Learning*, vol. 3, no. 1, pp. 1–122, 2011.
- [29] R. A. Jabr, "Radial distribution load flow using conic programming," *IEEE Trans. on Power Systems*, vol. 21, no. 3, pp. 1458–1459, 2006.
- [30] D. K. Molzahn, J. T. Holzer, B. C. Lesieutre, and C. L. DeMarco, "Implementation of a large-scale optimal power flow solver based on semidefinite programming," *IEEE Trans. on Power Systems*, vol. 28, no. 4, pp. 3987–3998, 2013.
- [31] E. Dall'Anese, H. Zhu, and G. B. Giannakis, "Distributed optimal power flow for smart microgrids," *IEEE Trans. on Smart Grid*, vol. 4, no. 3, pp. 1464–1475, Sep 2013.
- [32] S. H. Low, "Convex relaxation of optimal power flow Part I: Formulations and equivalence," *IEEE Trans. on Control of Network Systems*, vol. 1, no. 1, pp. 15–27, 2014.
- [33] B. A. Robbins, H. Zhu, and A. D. Domínguez-García, "Optimal tap setting of voltage regulation transformers in unbalanced distribution systems," *IEEE Trans. on Power Systems*, vol. 31, no. 1, pp. 256–267, Jan 2016.
- [34] L. Gan and S. H. Low, "Convex relaxations and linear approximation for optimal power flow in multiphase radial networks," in *Power Systems Computation Conference*, Wroclaw, Poland, Aug 2014.

- [35] E. Dall’Anese, S. Guggilam, A. Simonetto, Y. Chen, and S. Dhople, “Optimal regulation of virtual power plants,” *IEEE Trans. on Power Systems*, Aug. 2017.
- [36] D. Cohen, U. Shamir, and G. Sinai, “Optimal operation of multi-quality water supply systems-II: The QH model,” *Engineering Optimization*, vol. 32, no. 6, pp. 687–719, 2000.
- [37] B. Coulbeck, C. H. Orr, and A. E. Cunningham, “Ginas 5 reference manual,” *Research Rep*, vol. 56, 1991.
- [38] B. Ulanicki, J. Kahler, and B. Coulbeck, “Modeling the efficiency and power characteristics of a pump group,” *Journal of water resources planning and management*, vol. 134, no. 1, pp. 88–93, 2008.
- [39] N. Li, L. Chen, and S. H. Low, “Optimal demand response based on utility maximization in power networks,” in *2011 IEEE power and energy society general meeting*. IEEE, 2011, pp. 1–8.
- [40] M. Razaviyayn, “Successive convex approximation: Analysis and applications,” Ph.D. dissertation, University of Minnesota, 2014.
- [41] J. Löfberg, “YALMIP: A toolbox for modeling and optimization in MATLAB,” in *IEEE International Symposium on Computer Aided Control Systems Design*, 2004.
- [42] J. F. Sturm, “Using SeDuMi 1.02, a MATLAB toolbox for optimization over symmetric cones,” *Optimization methods and software*, vol. 11, no. 1-4, pp. 625–653, Jan 1999.